# Magnetohydrodynamic Activity in High-$\beta$, Currentless Plasmas in Heliotron-$E$

J. H. Harris
*Oak Ridge National Laboratory, Oak Ridge, Tennessee 37831*

and

O. Motojima, H. Kaneko, S. Besshou, H. Zushi, M. Wakatani, F. Sano, S. Sudo, A. Sasaki, K. Kondo, M. Sato, T. Mutoh, T. Mizuuchi, M. Iima, T. Obiki, A. Iiyoshi, and K. Uo
*Plasma Physics Laboratory, Kyoto University, Gokasho, Uji, Kyoto, Japan*
(Received 3 May 1984)

Electron-cyclotron and neutral-beam heating have been used to produce currentless plasma with $\langle\beta\rangle \approx (1\text{–}2)\%$ in the Heliotron-$E$ device. For moderately peaked profiles, magnetohydrodynamic activity that peaks at the $\iota = 1$ surface has been observed. The characteristics of the fluctuations are consistent with theoretical expectations for an $m = 1$ pressure-driven instability. The magnetohydrodynamic activity is associated with particle and energy losses but has not yet been directly linked to global confinement.

PACS numbers: 52.55.Ke, 52.35.–g

Stellarator/heliotron devices are attractive fusion reactor candidates because they offer the prospect of steady-state operation without plasma current, thus eliminating a major driving force for instabilities and the need for current drive. A critical parameter determining reactor feasibility is the maximum ratio of plasma pressure to magnetic field pressure, beta ($\beta = 2\mu_0 p/B^2$), that can be confined. This "beta limit" is likely to be influenced by magnetohydrodynamic (MHD) instabilities driven by the plasma pressure gradient.[1-7] In this Letter we report the first experimental observations of MHD activity in high-$\beta$, currentless plasmas in the Heliotron-$E$ device.

Heliotron-$E$ is a large device (major radius $R = 220$ cm, average plasma minor radius $\bar{a} = 20$ cm) with an $l = 2$, $m = 19$ helical field having high rotational transform ($\iota$) and shear.[8] For these experiments, the auxiliary toroidal field coils were not energized, so that the confining field was produced by the helical and vertical field coils alone. The vacuum field rotational-transform profile is then $\iota(\bar{r}/\bar{a}) = 0.55 + 1.95(\bar{r}/\bar{a})^4$; thus, the $\iota = 1$ surface lies at $\bar{r}/\bar{a} \approx 0.7$.

The high-$\beta$ experiments were performed at a toroidal field $B_T = 0.94$ T. Currentless target plasmas were produced with second-harmonic electron-cyclotron heating (ECH) using 100 to 300 kW of rf power from one or two 53.2-GHz Varian gyrotrons. Gas puffing was applied during the 40- to 50-ms ECH pulse to raise the average density $\bar{n}_e$ to $(1\text{–}2)\times 10^{13}$ cm$^{-3}$, at which time one 28° coinjecting neutral-beam line was turned on, followed by a perpendicular injector and an additional coinjector 30 to 40 ms later. Up to 2.4 MW of neutral power at an energy of 23–30 keV was thus injected into the torus. Gas puffing was used to raise the density further during injection to reduce shinethrough losses, and the plasma parameters during the high-$\beta$ portion of the discharge were typically $\bar{n}_e = (4\text{–}10)\times 10^{13}$ cm$^{-3}$, $T_{e0} = 300\text{–}500$ eV, $T_{i0} = 200\text{–}500$ eV, and $\tau_E$(gross) $\approx 10$ ms. In this Letter, we use central beta ($\beta_0$) and volume-averaged beta ($\langle\beta\rangle$) values based on profile measurements[8] with Thomson scattering, far-infrared (FIR) laser and 2-mm microwave interferometry, scanning charge-exchange neutral analysis, and Doppler broadening of impurity lines. To avoid excessive impurity influx due to large beam shinethrough power flux to the chamber wall, we operate at $\bar{n}_e > 4\times 10^{13}$ cm$^{-3}$. At these densities, we find that, as in high-density, high-$\beta$ tokamaks,[9] the fast ion contribution to the total pressure is small ($\lesssim 10\%$ for the present experiments), and so we neglect it in quoting $\beta$ values. In these experiments it was not possible to measure the finite-$\beta$ distortion of the rotational-transform profile caused by the Pfirsch-Schlüter currents,[1] so the vacuum profile is used for reference. This distortion is likely to be small since $\langle\beta\rangle$ is only (1–2)%, the rotational transform is quite large, and the heating phase is short ($\sim 100$ ms) compared to the magnetic diffusion time ($\gtrsim 1$ s).

For high-$\beta$ discharges with moderately peaked profiles and $\beta_0 \gtrsim 2\%$, characteristic fluctuations are observed on a number of diagnostics (see Fig. 1). Signals from a soft x-ray diode array show sawtooth oscillations accompanied by smaller sinusoidal fluctuations, which are qualitatively similar to the sawtooth oscillations seen in tokamaks.[10] The fall of the sawtooth coincides with spikes in the signals

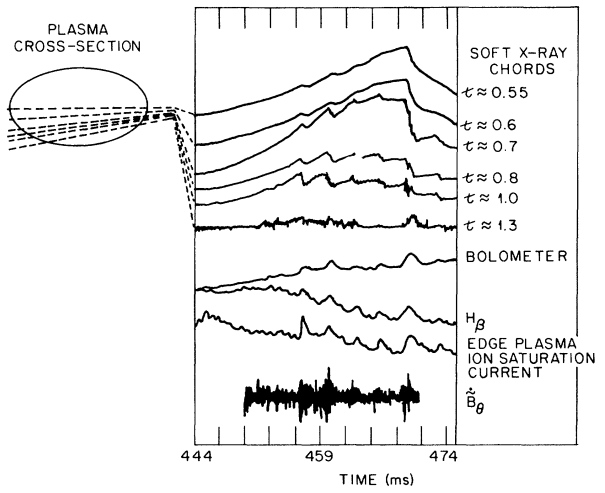


FIG. 1. Diagnostic signals for a high-$\beta$ Heliotron-$E$ discharge with sawteeth. The chordal soft x-ray signals are labeled with the $t$ values of their tangent magnetic surfaces. The last sawtooth (at $t \approx 469$ ms) is an internal disruption.

from the uncollimated (total power) bolometer, the hydrogen $H_\beta$-line monitor, and the edge plasma ion-saturation-current probes and with bursts in the poloidal magnetic field fluctuations ($\tilde{B}_\theta$) measured by Mirnov coils at the vacuum chamber wall. During the bursts, the quantity $\tilde{B}_\theta(\text{wall})/B_\theta(t=1)$ reaches $\sim 1\%$; here $B_\theta(t=1) = (0.7\bar{a}/R)B_T$ is the calculated vacuum poloidal field at the $t=1$ surface and is used for convenience. Soft x-ray and FIR interferometer measurements of the temperature and density changes during a sawtooth crash show that $\beta_0$ and $\langle\beta\rangle$ decrease by $\sim (5\text{–}10)\%$; the bolometer spikes show an increased power loss, which is consistent with this finding. The spikes in edge diagnostic signals ($H_\beta$ and ion saturation current) are further evidence of particle and energy losses. The strongest sawteeth end in what we call internal disruptions, in which the soft x-ray emission (which varies approximately as $n_e^2 T_e^{7/2}$) from chord radii inside the vacuum field $t=1$ surface falls sharply [by $\sim (10\text{–}50)\%$], while the emission from chords outside $t=1$ rises [Fig. 2(a)]. Third-harmonic electron-cyclotron–emission measurements[11] of electron temperature and density also show that these internal disruptions result in the appearance of a heat pulse[12] in the region $\bar{r}/\bar{a} \gtrsim 0.7$. So far, we have not found coherent oscillations in the fast-ion charge-exchange flux like those associated with fast-ion losses induced by MHD activity in the PDX tokamak.[13]

The profile of the normalized x-ray emission amplitude $\Delta\tilde{X}/X$ of the 2- to 5-kHz oscillations that accompany the sawteeth rises sharply near the radius of the $t=1$ surface [Fig. 2(b)]. The relative phase of these oscillations is odd about the plasma center (Fig. 3), as expected for an instability with poloidal mode number $m=1$, and the disturbance propagates poloidally in the electron diamagnetic drift direction. The $m=1$ mode assignment is supported by additional fluctuation measurements with the multichord FIR interferometer. Phase measurements with torodially separated diagnostics are consistent with a toroidal mode number $n=1$; this finding is corroborated by the peaking of the $m=1$ fluctuation amplitude near $t=1$.

During a sawtooth, the $m=1$ oscillations increase in amplitude, with a typical growth rate $\gamma$

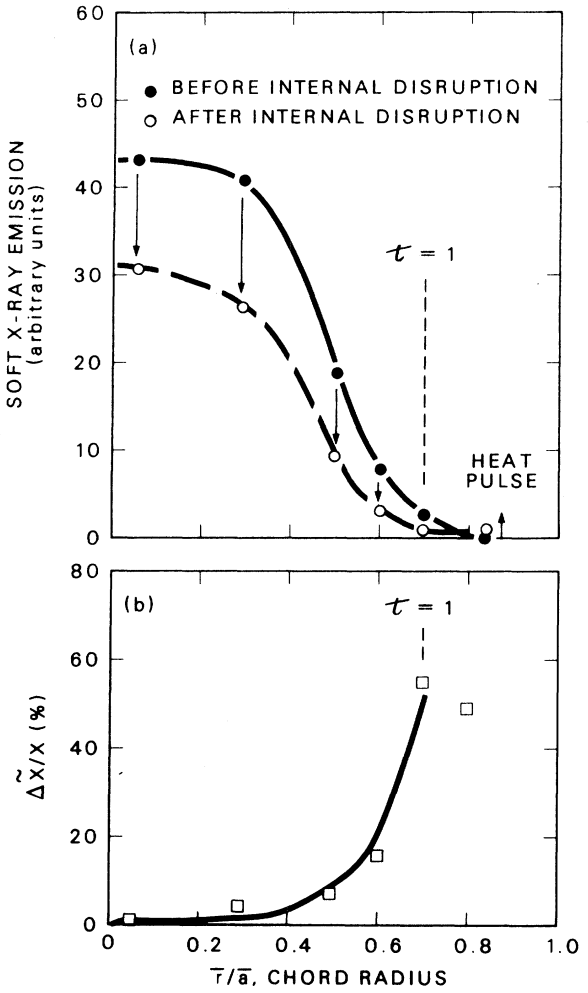


FIG. 2. Profiles of soft x-ray signal amplitude as a function of detector chord radius (average radius of tangent magnetic surface): (a) total signal amplitude before and after large sawtooth (internal disruption) and (b) normalized sinusoidal precursor oscillation amplitude ($\Delta\tilde{X}/X$) just before internal disruption.

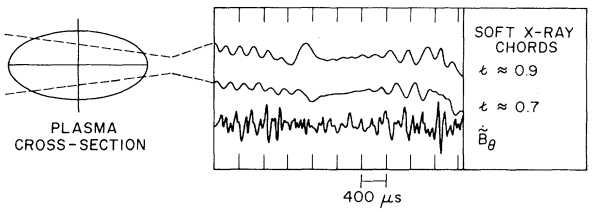


FIG. 3. Time expansion of soft x-ray and Mirnov-loop ($\dot{\tilde{B}}_\theta$) signals during successive $m=1$ instability cycles.

$\sim (1\text{–}3)\times 10^3$ s$^{-1}$, and are well correlated with growing oscillations on the Mirnov-coil signal (Fig. 3). An additional component at twice the $m=1$ frequency is usually present in $\dot{\tilde{B}}_\theta$, and is most probably due to an $m=2$, $n=2$ instability component, whose apparent relative amplitude is enhanced by the time derivative in $\dot{\tilde{B}}_\theta$.

The amplitude of the sawtooth oscillations depends on $\beta$, with a threshold of $\beta_0 \approx 2\%$ (Fig. 4). Here we have plotted the sawtooth amplitude against central-$\beta$ values because they can be obtained directly from central temperature and density measurements. The other signals associated with the sawteeth—bursts in $\dot{\tilde{B}}_\theta$ and spikes on edge diagnostics—show essentially the same threshold behavior.

Theoretical studies of the ideal MHD stability of the Heliotron-$E$ configuration have been carried out with use of different methods,[1-7] and the conclusions generally agree. The most serious instability for Heliotron-$E$ is the pressure-driven $m=1$, $n=1$ interchange mode resonant at the $\iota=1$ surface, which falls in a region of unfavorable average curvature. These calculations yield critical $\beta$ values of $\beta_0 \approx (2\text{–}5)\%$, depending on the pressure profile used. Of course, a direct comparison of the experimental results with ideal MHD theory is simplistic, since resistive effects are likely to be important at these temperatures ($T_e < 500$ eV). To study resistive pressure-driven instabilities and follow their nonlinear development, we have modified our resistive MHD code[14] to include finite-pressure effects.

For discharges near the threshold, where weak MHD activity is observed (see Fig. 4), we have used the method of Wakatani[5] with pressure profiles derived from experimental measurements (Fig. 5) to determine that the plasma is ideally stable to the $m=1$, $n=1$ mode. When resistivity is included, the mode is weakly unstable but does not significantly alter the pressure profile; this is consistent with the observation of only weak MHD oscillations. These findings are unchanged when a

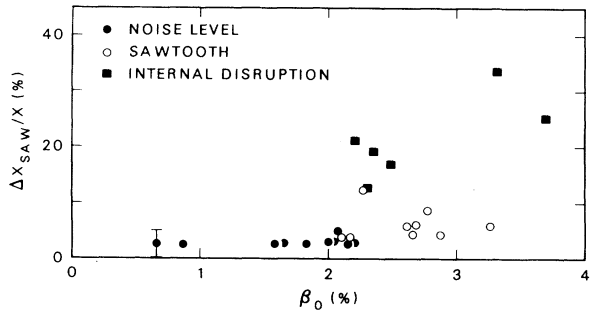


FIG. 4. Central-chord soft x-ray sawtooth amplitude ($\Delta X_{saw}/X$) as a function of central $\beta$ ($\beta_0$) for discharges with moderately peaked profiles. For $\beta_0 < 2\%$, only weak noise fluctuations are observed.

pressure profile based on the assumption $T_i(\bar{r}) = T_e(\bar{r})$ [rather than the measured $T_i(\bar{r})$] is used in the analysis. At higher $\beta$, our nonlinear resistive MHD simulations[15] show a breakup of magnetic surfaces near $\iota=1$, the formation of island structures similar to those seen in tokamaks,[10] and substantial deformations of the pressure profile. Simulations of the soft x-ray wave forms for these stronger instabilities show many of the features observed in higher-$\beta$ discharges. These results suggest that the resistive interchange mode is an attrac-

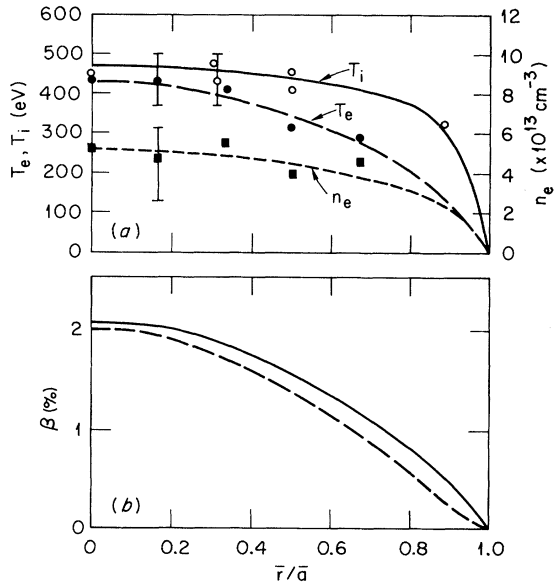


FIG. 5. Profiles for a discharge at the threshold for the onset of MHD activity ($\beta_0 \approx 2.1\%$, $\langle\beta\rangle \approx 1\%$): (a) temperature and density profiles (charge-exchange and single-shot Thomson-scattering measurements); (b) $\beta(\bar{r})$ profiles derived from fits to experimental data. In (b) the $T_i$ profile was used for the solid curve, while the assumption $T_i(\bar{r}) = T_e(\bar{r})$ was used for the dotted curve.

tive explanation for the instabilities seen in the experiment.

Power-balance studies of high-$\beta$ discharges[16] indicate that the MHD activity does not now play a significant role in global energy confinement. The plasma parameters are at present limited by large impurity radiation losses—in some cases $\gtrsim 50\%$ of the input power. Nevertheless, the highest $\langle\beta\rangle$ values ($\approx 2\%$) have been achieved in discharges in which the MHD activity is absent or greatly reduced.[16] In these "$Q$-mode" (quiet) discharges, increased gas puffing results in a pressure profile that is significantly broader than that in the "$S$-mode" (sawtooth) discharges; theoretical studies[5,16] suggest that these broad profiles should be more stable to the pressure-driven mode.

In summary, we have made the first observations of MHD activity in a high-$\beta$ toroidal plasma confined with external rotational transform and zero induced current. The characteristics of the $m=1$ mode that is observed generally coincide with theoretical expectations for a pressure-driven instability in the high-shear, high-transform Heliotron-$E$ configuration. Specific particle and energy losses are associated with the MHD oscillations, but a direct link between MHD activity and global confinement has not yet been observed.

We gratefully acknowledge the assistance of I. Ohtake and the Heliotron-$E$ operating team. One of us (J.H.H.) participated in these experiments during a U.S.–Japan fusion research exchange. This work was supported in part by the Office of Fusion Energy, U.S. Department of Energy, under Contract No. DE-AC05-84OR21400 with Martin Marietta Energy Systems, Inc.

[1]G. Anania and J. L. Johnson, Phys. Fluids **26**, 3070 (1983).

[2]V. D. Shafranov, Phys. Fluids **26**, 357 (1983).

[3]F. Bauer, O. Betancourt, and P. Garabedian, *Magnetohydrodynamic Equilibrium and Stability of Stellarators* (Springer, New York, 1984).

[4]H. R. Strauss and D. Monticello, Phys. Fluids **24**, 1148 (1981).

[5]M. Wakatani, IEEE Trans. Plasma Sci. **9**, 243 (1981); M. Wakatani *et al.*, J. Phys. Soc. Jpn. **47**, 974 (1979).

[6]L. M. Kovrizhnykh and S. V. Shchepetov, Nucl. Fusion **23**, 859 (1983).

[7]B. A. Carreras *et al.*, Phys. Fluids **26**, 3569 (1983).

[8]K. Uo *et al.*, in *Proceedings of the Ninth International Conference on Plasma Physics and Controlled Nuclear Fusion Research, Baltimore, 1982* (International Atomic Energy Agency, Vienna, 1983), Vol. 2, p. 209; Heliotron-$E$ Staff, Kyoto University Plasma Physics Laboratory Reports No. PPLK-2, 1981 (unpublished), and No. PPLK-4, 1983 (unpublished); K. Uo, Plasma Phys. **13**, 243 (1971), and Nucl. Fusion **13**, 661 (1973).

[9]G. H. Neilson *et al.*, Nucl. Fusion **23**, 285 (1983).

[10]J. L. Dunlap *et al.*, Phys. Rev. Lett. **48**, 538 (1982).

[11]J. N. Talmadge *et al.*, Phys. Rev. Lett. **52**, 33 (1984).

[12]J. D. Callen and G. L. Jahns, Phys. Rev. Lett. **38**, 491 (1977).

[13]K. McGuire *et al.*, Phys. Rev. Lett. **50**, 891 (1983).

[14]M. Wakatani *et al.*, Nucl. Fusion **23**, 1669 (1983).

[15]K. Uo *et al.*, in Proceedings of the Tenth International Conference on Plasma Physics and Controlled Nuclear Fusion Research, London, September 1984 (to be published).

[16]O. Motojima *et al.*, in *Proceedings of the Fourth International Symposium on Heating in Toroidal Plasmas, Rome, 1984* (International School of Plasma Physics, Varenna, 1984), Vol. 2, p. 865; O. Motojima *et al.*, to be published.